Past, Present, and Future of Annexin A5: From Protein Discovery to Clinical Applications*

Hendrikus H. Boersma, PharmD[1,2]; Bas L.J.H. Kietselaer, MD[3]; Leo M.L. Stolk, PharmD, PhD[2]; Abdelkader Bennaghmouch, MD[3]; Leonard Hofstra, MD, PhD[3]; Jagat Narula, MD, PhD[4]; Guido A.K. Heidendal, MD, PhD[1]; and Chris P.M. Reutelingsperger, PhD[5]

[1]Department of Nuclear Medicine, Maastricht University Hospital, Maastricht, The Netherlands; [2]Department of Clinical Pharmacy and Toxicology, Maastricht University Hospital, Maastricht, The Netherlands; [3]Department of Cardiology, Cardiovascular Research Institute, Maastricht University, Maastricht, The Netherlands; [4]Cardiology Division, UCI Medical Center, Orange, California; and [5]Department of Biochemistry, Cardiovascular Research Institute, Maastricht University, Maastricht, The Netherlands

In this article, we review the clinical aspects of imaging with the programmed cell–detecting protein annexin A5 (anxA5). AnxA5 binds to phosphatidylserine, which is one of the "eat me" signals at the surface of the apoptotic cell. This biologic property forms the basis for the development of anxA5 as a diagnostic tool. Within this context, the clinical relevance, limitations, and future perspectives of this approach of visualizing cell death are discussed in this article, as are other potential applications of anxA5. Furthermore, the biologic properties and the radiopharmaceutical, pharmacologic, and biodistribution aspects of anxA5 are reviewed and discussed in this article. Radiolabeled anxA5 bears the promise of becoming a clinically applied radiopharmaceutical with potential applications in cardiology and oncology. Visualization of cell death is important in pathologies such as myocardial infarction, atherosclerosis, and cancer. Furthermore, radiolabeled anxA5 may be developed as a tool for monitoring cell death–inducing or cell death–preventing therapies. In addition, experiences with radiolabeled anxA5 open novel avenues for drug targeting with anxA5 as a biologic "cruise missile."

Key Words: annexin A5; diagnostic tool; radiopharmaceutical; clinical applications; cardiovascular disease; cancer

J Nucl Med 2005; 46:2035–2050

Apoptosis or programmed cell death (PCD) plays an important role not only in physiology but also in pathology. For example, acute myocardial infarction is associated with PCD of cardiomyocytes (*1,2*). Furthermore, the vulnerability of atherosclerotic lesions is determined by the number of apoptotic cells present (*3*). Also, many drugs, such as cytostatic agents, induce a therapeutic effect through the activation of PCD in target cells (*4*). Therefore, the detection and quantification of apoptosis in vivo are of significant clinical value for diagnosis and assessment of therapeutic efficacy.

In the last decade, a molecular imaging (MI) protocol was established to measure PCD in vitro and in vivo in animal models and patients (*2,5–7*). This imaging protocol is based on the facts that apoptotic cells externalize the negatively charged phospholipid phosphatidylserine (PS) and that the human protein annexin A5 (anxA5) binds to PS selectively and with a high affinity (*8*).

This review highlights the different aspects of this technique as a diagnostic tool and discusses the clinical relevance, limitations, and future perspectives of this approach. The biochemical properties of anxA5 as well as its radiopharmaceutical aspects and biodistribution properties also are reviewed.

PAST: DISCOVERY OF ANXA5

AnxA5 is a member of the annexin family. This is a multiprotein family of over 160 proteins that share the property of Ca^{2+}-dependent binding to negatively charged phospholipid surfaces (*9*). At the end of the 1970s, anxA5 was first isolated from human placenta (*10*). A few years later, the protein (Fig. 1) was discovered independently in blood vessels and named vascular anticoagulant protein alpha (VAC-α) because of its property to inhibit blood coagulation (*11*). The anticoagulant mechanism is based on the high-affinity binding to PS. This property makes anxA5 very effective in inhibiting the prothrombinase complex (mean ± SD 50% inhibitory concentration, 16 ± 12 nmol/L) (*12*). Further information on the biophysical, biochemical, and biologic properties of anxA5 and other, related proteins is provided in several excellent reviews (*9,13–16*). Elucidation of its primary structure revealed that VAC-α was a member of the annexin family. It was therefore termed annexin V. During the last decade, more than

Received Mar. 17, 2005; revision accepted Sep. 23, 2005.

For correspondence contact: Hendrikus H. Boersma, PharmD, Department of Clinical Pharmacy and Toxicology, Maastricht University Hospital, P.O. Box 5800, NL-6202 AZ Maastricht, The Netherlands.

E-mail: hboe@kfls.azm.nl

*NOTE: FOR CE CREDIT, YOU CAN ACCESS THIS ACTIVITY THROUGH THE SNM WEB SITE (http://www.snm.org/ce_online) THROUGH DECEMBER 2006.

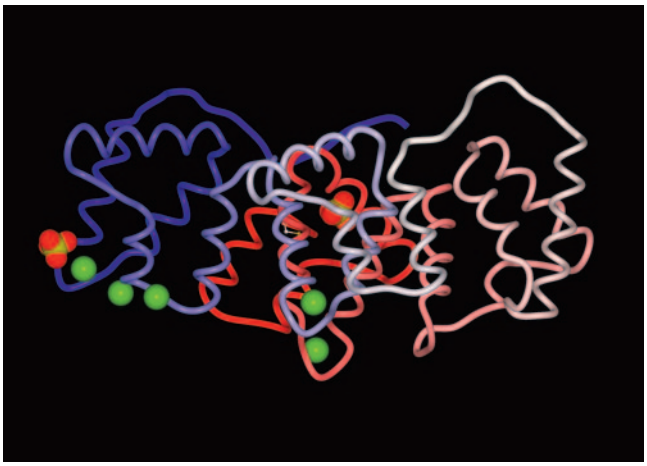

FIGURE 1. X-ray analysis revealed the tertiary structure of anxA5, as depicted here. The protein consists of 319 amino acids. Molecule is arranged in planar cyclic structure of 4 domains, which are indicated by different colors in structure. Also shown are Ca^{2+} ions (green spheres).

100 annexin family members have been discovered (*16*). These discoveries have led to a further adaptation of the annexin nomenclature by the introduction of 5 major annexin groups (A–E) (*9*). According to this system, human annexin V was renamed anxA5. After its discovery, anxA5 was produced by the expression of its complementary DNA in the bacterium *Escherichia coli* (*17–19*). Most studies have used this recombinant form of anxA5.

DEVELOPMENT OF ANXA5 AS DIAGNOSTIC TOOL

Apoptosis, which is the major form of PCD (*4*), plays an important role in the development, homeostasis, and disease of an organism. In pathology, 2 opposing situations can arise concerning apoptosis: 1 situation in which there is abundant apoptosis, as in cases of transplanted organ rejections, AIDS, septic shock, and cardiovascular and neurodegenerative diseases, and 1 situation in which there is insufficient apoptosis, as in cases of cancer (*20*).

In 1992, Fadok et al. (*21*) revealed that PS is expressed on the cell surface of apoptotic cells (*21*). Viable cells retain PS predominantly located in the inner leaflet of the cell membrane (*22*). This notion led Koopman et al. (*8*) and others to design an apoptosis detection assay on the basis of fluorescence (fluorescein isothiocyanate)-labeled anxA5 (*8,23–25*). To be able to discern between apoptotic cells and necrotic cells, which have compromised plasma membrane integrity, propidium iodide (PI) was added. By this means, viable, apoptotic, and necrotic cells can be discriminated by either fluorescence microscopy (Fig. 2) or flow cytometry. PCD is a rapidly changing topic. The current state of the art concerning apoptosis is described in several recent reviews (*4,26–32*).

The anxA5 affinity assay was further developed by labeling anxA5 with biotin or with radionuclides to enable various protocols for measuring apoptosis in vitro (*33*) and in vivo in animal models (*5–7,34–38*). The availability of ^{99m}Tc-anxA5 produced under Good-Manufacturing-Practice regulations led to the possibility of studying apoptosis in patients noninvasively (*2,39–43*).

PRESENT: RADIOPHARMACEUTICAL ASPECTS OF ANXA5

Radiolabeled Derivatives of AnxA5

Here we describe the state of the art of research with anxA5 as a diagnostic tool. First, the radioisotopes, their conjugation methods, and quality control of the radiopharmaceuticals are described. The main features, advantages, and disadvantages of the isotopes used and the corresponding radiopharmaceuticals are shown in Table 1.

Technetium-Labeled AnxA5

^{99m}Tc is a radionuclide with good properties for diagnostic purposes. The complicated radiochemistry of ^{99m}Tc can be regarded as one of its disadvantages. Unlike the situation with halogens, such as ^{123}I and ^{18}F, it is not possible to replace a hydrogen atom with a technetium ion, nor can it serve as a substitute for the commonly available carbon,

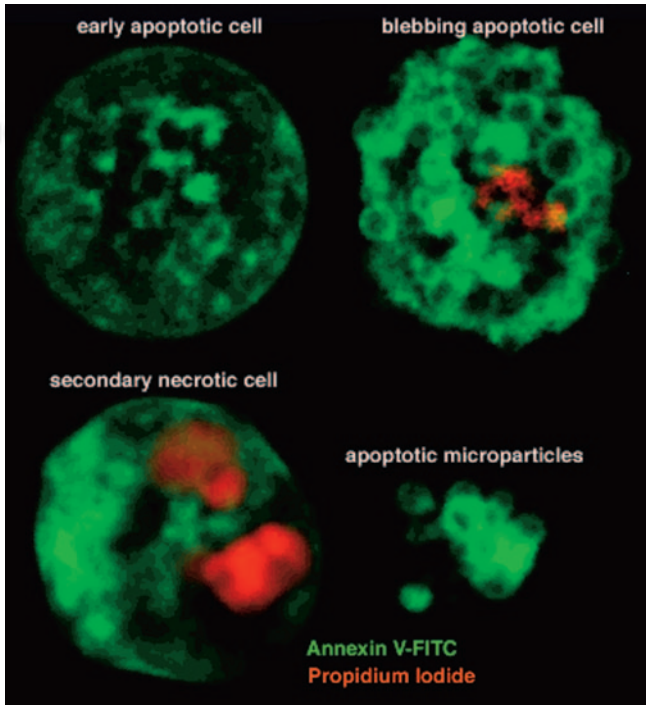

FIGURE 2. AnxA5 is able to bind to cells in all stages of cell death program. Shown are Fas (D95) ligand–stimulated Jurkat cells. (Top left) Early stage of cell death. Fluorescent anxA5 (green) binds to outer cell membrane. (Top right) Cell in later phase showing binding of PI (red), which is intercalated with DNA and anxA5. Binding of PI is indicative of disintegration of cell membrane. Also, formation of apoptotic bodies is visible. (Bottom) Final stage of PCD. Here, only anxA5 binding to cellular membrane residues can be observed. Also shown is cell undergoing secondary necrosis after PCD. AnxA5 uptake is still present, but cell structures are different from those of cells undergoing PCD only.

TABLE 1
Features, Advantages, and Disadvantages of Isotopes and Radiopharmaceuticals

Radiopharmaceutical	Emissions and energy	Physical half-life	Advantages (Pro) or Disadvantages (Con)
^{99m}Tc-AnxA5 (general)	γ, 140.5 keV	6.02 h	Pro: ^{99m}Tc can be obtained easily at low cost by use of ^{99}Mo/^{99m}Tc generators; excellent imaging properties Con: difficult radiochemistry for technetium; biodistribution influenced by conjugation method
^{99m}Tc-Imino-anxA5	γ, 140.5 keV	6.02 h	Pro: labeling can be performed easily Con: RCP ≈ 80%; high uptake of radiopharmaceutical in liver, kidneys, and spleen; long biologic half-life
^{99m}Tc-BTAP-anxA5	γ, 140.5 keV	6.02 h	Pro: RCP > 93%; short biologic half-life Con: labeling method very laborious; high radioactivity uptake in liver, kidneys, spleen, and abdomen; low radiochemical yield
^{99m}Tc-HYNIC-anxA5	γ, 140.5 keV	6.02 h	Pro: labeling method well established; prefabricated kit, so labeling can be performed easily Con: high uptake of radiopharmaceutical in kidneys and liver; long biologic half-life
^{99m}Tc-EC-anxA5	γ, 140.5 keV	6.02 h	Pro: prefabricated kit, so labeling can be performed easily Con: to establish this method, more research is required
^{94m}Tc-AnxA5 (general)	β^+, 2.5 MeV	53 min	Pro: easiest way to transform SPECT into PET; when HYNIC-anxA5 is used, labeling can be performed easily Con: difficult radiochemistry for technetium; biodistribution influenced by conjugation method; expensive and difficult to obtain
^{123}I-AnxA5	γ, 160 keV	13 h	Pro: no uptake in liver and kidneys after 12 h; good imaging expected in abdominal region, compared to that with known ^{99m}Tc compounds; good radiochemical purity Con: laborious labeling method; more expensive than ^{99m}Tc labeling
^{124}I-AnxA5	β^+, E = 1.53, 2.14 MeV, γ (complex decay under emission of several high-energy γ-photons)	4.2 d	Pro: long-lived PET tracer; suitable for animal studies and studies in humans with terminal disease; labeled compound with long shelf-life (4 d without detectable deiodination); RCP > 95% Con: high radiation burden and therefore less suitable for patient imaging; laborious labeling method
^{125}I-AnxA5	EC, 35 keV	60 d	Pro: long-lived isotope; very useful for research purposes to test iodine labeling techniques in animals; low radiation burden for research workers Con: no imaging possibility
^{111}In-AnxA5	γ, 173 keV, 247 keV (ratio of both energies is 1:1), electron capture gives x-ray energy of 23 keV	2.8 d	Pro: longer-lived isotope; may be suitable for imaging of tumor response in patients Con: difficult radiochemistry for indium; biodistribution influenced by conjugation method; biodistribution of pegylated In-conjugated anxA5 appears to be poor; rather high radiation burden in patients
^{18}F-AnxA5	β^+, 633 keV	110 min	Pro: PET tracer with optimal half-life for imaging; promising agent for patient imaging Con: more research is required to establish its use in patients; labeling method is not yet standardized

nitrogen, or oxygen atoms (*44*). Therefore, technetium requires a more complex conjugation principle to attach the atom to bioactive molecules. Predominantly, the latter has been achieved by use of bifunctional chelating agents. Several methods have been used to label anxA5: ester bonds (MAG3, dithiolate), amide bonds (hydrazinonicotinamide [HYNIC]), and thiolate bonds (iminothiolane) (*45*).

Preliminary data are available on the use of another isotope of technetium, ^{94m}Tc, as a PET probe for the labeling of HYNIC-anxA5. Because of its half-life and favorable positron energy (Table 1), its use as a PET radiopharmaceutical seems very attractive (*45*). Labeling methods for technetium are well established. A major problem with the use of technetium for PET in clinical studies may be the quality of the images compared with that of SPECT images. The biodistribution of HYNIC-anxA5 is unfavorable for imaging shortly after injection, as would be the case with ^{94m}Tc-HYNIC-anxA5, because of the shorter half-life of this isotope. It is possible that other labeling methods with ^{94m}Tc will produce better results in clinical practice.

*^{99m}Tc-(*N*-1-Imino-4-Mercaptobutyl)-AnxA5.* Initially, we started to perform imaging with anxA5 by using ^{99m}Tc-(*N*-1-imino-4-mercaptobutyl)-anxA5 (^{99m}Tc-imino-anxA5). This conjugation method was developed at Mallinckrodt and commercially used to label human immunoglobulin for the detection of inflammation (*46*). Iminothiolane converts free amino groups in the anxA5 molecule into free sulfhydryl groups. These can bind technetium in the presence of stannous ions. To achieve labeling of acceptable quality, a long incubation time (2 h) is necessary. The obtained radiochemical purity was acceptable but low (Table 1) (*43*). Furthermore, the radiopharmaceutical labeling efficiency decreased from 83% to 76% during the shelf life of the radiolabeling kit (*43*). The latter problem forced us to search for a more accurate labeling procedure. Nonetheless, ^{99m}Tc-imino-anxA5 was the first nuclear probe that was used to image apoptosis in humans (*2,47*).

^{99m}Tc-(4,5-Bis(Thioacetamido)Pentanoyl) (BTAP)-AnxA5. We investigated the use of ^{99m}Tc-BTAP-anxA5. ^{99m}Tc labeling of anxA5 was achieved by synthesis of an activated diamide dimercapride N_2S_2 compound, followed by conjugation to human recombinant anxA5 and labeling with ^{99m}Tc. BTAP-anxA5 was purified by chromatography on a PD-10 column (Theseus Imaging Corp.) before injection (*43,48,49*). The entire preparation procedure took about 75 min. The fluctuating and low radiochemical yield (10%–25%) depended predominantly on the specific radioactivity of the eluate used (Table 1) (Hendrikus H. Boersma, Guido A. K. Heidendal, Chris P.M. Reutelingsperger, unpublished data, April 2002). This method of ^{99m}Tc labeling was previously developed as the Onco Trac method to label Fab′ fragments for tumor detection (*50*).

^{99m}Tc-Ethylenedicysteine (EC)-AnxA5. Another N_2S_2 method for labeling anxA5 with technetium makes use of EC as a linker (*51*). EC-treated anxA5 can be labeled with ^{99m}Tc in the presence of stannous chloride. With this labeling method, a radiochemical purity (RCP) of approximately 100% was achieved. This method appears to be an adequate and efficient way to label anxA5 with technetium, but additional investigations are required (*51*).

^{99m}Tc-HYNIC-AnxA5. The HYNIC conjugation method for labeling anxA5 with ^{99m}Tc has been the most widely applied method for clinical studies to date. So far, ^{99m}Tc-HYNIC-anxA5 has been proven to be the main ^{99m}Tc-anxA5 radiopharmaceutical. It is available as a preformulated radiolabeling kit with a long shelf life. In the presence of stannous ions and with tricine (Theseus Imaging Corp.) as a coligand, use of the kit results in HYNIC-anxA5 with a radiochemical purity of >90%, without requiring additional purification (*52*). Labeling is a 1-step reaction, with 30 min of incubation at ambient temperature being the most time-consuming step. It requires about 1 GBq of ^{99m}Tc, which is about 25% of the radioactivity needed for the preparation of BTAP-anxA5 (*52,53*).

Novel Labeling Methods with ^{99m}Tc Binding AnxA5 Mutant Proteins. To simplify the preparation and labeling of anxA5 for imaging purposes, the addition of peptide sequences that will directly form endogenous chelation sites for ^{99m}Tc was investigated. Three anxA5 mutants, named annexin V-116, annexin V-117, and annexin V-118, were constructed with N-terminal extensions of 7 amino acids containing either 1 or 2 cysteine residues and expressed in *E. coli*. The biopotency of these anxA5 mutants was shown to be conserved. With stannous chloride as the reducing agent and glucoheptonate as the exchange agent, all 3 proteins could be labeled with ^{99m}Tc. The membrane binding activity of the labeled proteins was shown to be comparable to that of wild-type anxA5. The labeling reaction was rapid, reaching a maximum of approximately 93% RCP after 40 min at room temperature (*54,55*). AnxA5 could be modified near its N terminus to incorporate sequences that form specific chelation sites for ^{99m}Tc without alteration of its high affinity for cell membranes (*54*).

Similarly, whether the novel ^{99m}Tc-carbonyl labeling method would be suitable for anxA5 also was investigated. Two mutants of anxA5, annexin V-122 and annexin V-123, were constructed with N-terminal extensions containing either 3 or 6 histidine residues. Both mutant proteins retained full binding affinity for cell membranes with exposed PS. With the ^{99m}Tc-carbonyl reagent, both proteins could be labeled with ^{99m}Tc to specific activities of at least 3.7–7.4 MBq/μg, with full retention of bioactivity (*55*).

Recently, Tait et al. (*56*) reported that the biodistribution of anxA5 is influenced by the labeling method and the Ca^{2+} binding sites of the molecule. For example, anxA5 mutant 128, with endogenous ^{99m}Tc chelation sites, is taken up by apoptotic cells to an extent similar to or better than that of HYNIC-anxA5. Furthermore, they showed that anxA5 mutant 128 had much lower renal uptake at 60 min after injection. The latter was suggested to be attributable to more rapid urinary excretion of radioactivity for anxA5 mutant 128 (*56*).

Tait et al. (*56*) further showed that the clearance from blood of anxA5 was not affected by its overall net charge and affinity of binding to PS. On the basis of their results, they postulated that clearance by the kidneys was a PS-independent process, whereas uptake in normal liver and spleen decreased with the PS affinity of the changed anxA5 molecule. The same pattern was observed in animals treated with cycloheximide to induce apoptosis. Control experiments with charge mutants showed that the effects seen with the affinity mutants were not attributable to the concomitant change in molecular charge that occurs in these mutants. They concluded that all 4 domains of anxA5 are required for optimal uptake in apoptotic tissues. AnxA5 derivatives with only 1 or 2 PS binding sites are unlikely to be suitable for imaging of cell death in vivo. They suggested that uptake in normal liver and spleen is specific whereas renal uptake is nonspecific (*56*).

AnxA5 Labeled with Halogen Radioisotopes

Most halogens used in radiolabeling are suitable for conjugation with anxA5. Labeling of anxA5 with ^{123}I, ^{124}I, and ^{18}F has been described and extends the possibilities for the use of radiolabeled anxA5 further toward PET as well as other SPECT applications.

^{123}I/^{124}I/^{125}I-Labeled AnxA5. Actually, the first method described for labeling anxA5 radioactively was iodination with ^{125}I and later with ^{123}I (*57*). At that time, anxA5 was used as a thrombus-identifying agent because its use as an apoptotic cell imaging probe had not yet been revealed.

Several types of iodination of anxA5 with ^{123}I and ^{125}I have been described. The efficiency of IODO-BEADS (Pierce) iodination was just below 30%; with the Bolton-Hunter protocol (*58*), 40% efficiency was achieved. Recently, Lahorte et al. (*59*) developed a slightly modified IODO-GEN (Pierce) method (*59,60*) to obtain ^{123}I-anxA5 (Table 1). The apparently favorable biodistribution properties render this labeled anxA5 suitable for imaging of the kidneys (*59*).

^{124}I-AnxA5 is currently under investigation as a PET probe. The relatively long half-life (Table 1) makes ^{124}I more suitable for in vitro experiments and animal studies than for clinical studies. Several methods for ^{124}I labeling of anxA5 have been described (*45*). Glaser et al. (*37*) compared the direct and common chloramine-T procedure with the indirect ^{124}I-m-*N*-succinimidyl-3-iodobenzoate (SIB)-labeling method. The authors showed that the ^{124}I-m-SIB-labeling method yielded ^{124}I-anxA5 with better binding properties than the chloramine-T procedure (*37*).

^{18}F-Labeled AnxA5. ^{18}F is a radioisotope with a favorable half-life (Table 1) for PET imaging in humans. Zijlstra et al. (*61*) developed an indirect labeling method for conjugating anxA5 with ^{18}F by use of *N*-succimidyl-4-^{18}F-fluorobenzoate (*61*). ^{18}F-AnxA5 appeared to behave in in vitro binding studies in a manner similar to that of unlabeled anxA5. The disadvantage of an indirect labeling method with ^{18}F is the short half-life of the isotope, which requires large initial amounts of radioactivity to start the production of the compound to obtain sufficient activity for imaging purposes (*61*).

Indium-Labeled AnxA5: ^{111}In-Polyethylene Glycol (PEG)-AnxA5

Recently, a method was developed to conjugate ^{111}In to anxA5. ^{111}In has the advantage of a physical half-life longer than that of ^{99m}Tc. Furthermore, an attempt was made to extend the biologic half-life of anxA5 by adding a PEG (molecular weight, approximately 3,400) moiety to the molecule (*62*). No human studies have been performed yet.

Quality Control of Radiolabeled AnxA5

Quality control of radiolabeled anxA5 in a clinical setting is generally performed by thin-layer chromatography or column chromatography. These methods, however, are able to determine only whether the labeling procedure was accurate and do not provide information about the biologic properties of labeled anxA5. We have developed a rapid and simple quality control method with PS-coated paramagnetic beads. AnxA5 binds to these beads with a high affinity in the presence of Ca^{2+} ions. The bead assay is specific, stability-indicating, repeatable, and reproducible. It allows determination within 25 min of the biologically active fraction of a radiolabeled (e.g., ^{99m}Tc, ^{123}I, or ^{18}F) anxA5 preparation (*52*).

Imaging Applications for AnxA5 in Animal Studies

The concept that anxA5 binds to apoptotic cells in the presence of Ca^{2+} was first proven in vitro with immortalized cell lines. These results were obtained with apoptotic Jurkat cells (*23*). The question remained, however, as to what would happen to cells during PCD in the complexity of the living organism. To test this concept, several animal models were developed to study the ability of anxA5 to bind to cells undergoing PCD in the complexity of the whole organism.

Myocardial Ischemia and Reperfusion. PCD is hardly detectable in adult organisms because of the efficient clearance of the dying cells by phagocytes. The situation differs completely in pathologies in which the clearance capacity is insufficient to remove all of the dying cells. Such a situation arises, for example, in the heart after ischemia or reperfusion injury. A mouse model was developed to mimic the human situation of an acute myocardial infarction that is treated with reperfusion therapy. The model consists of the ligation of the left anterior descending artery to apply ischemia. After a specified period of time, the ligation is removed to achieve reperfusion (*5,6*). Before or just after the end of the period of ischemia, either biotin-labeled (Fig. 3) or fluorescence-labeled (e.g., Oregon green) anx5A is injected intravenously into the mouse. Using this model, Dumont et al. (*5,6*) showed that labeled anxA5 stained the dying cardiomyocytes in the area at risk, while the living cardiomyocytes remained unstained.

Taki et al. (*63*) reported similar results with ^{99m}Tc-anxA5. This group studied the evolution of cell death after restora-

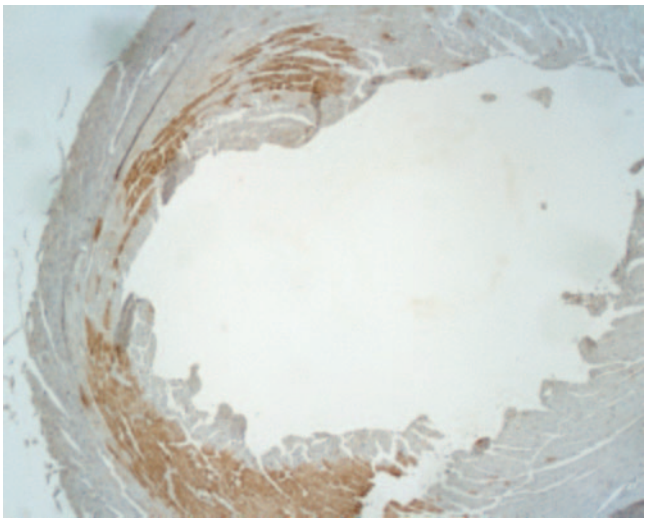

FIGURE 3. Transverse section of murine heart after 30 min of ischemia and 12 h of reperfusion. Cells were stained for presence of biotinylated anxA5.

tion of the blood flow by using anxA5 methodology. They studied groups of rats after a 20-min interval of coronary occlusion and reperfusion. Dual-tracer autoradiography (^{99m}Tc-anxA5/^{201}Tl) was performed to assess both ^{99m}Tc-anxA5 uptake and the area at risk. High ^{99m}Tc-anxA5 uptake was observed in the middle myocardium after 0.5–1.5 h of reperfusion. The area of anxA5 uptake expanded throughout the myocardium until 6 h after reperfusion and then gradually lessened over 3 d. Together, these data show that in mice, PCD commences soon after the onset of ischemia and gradually expands within the area at risk after reperfusion. A similar pattern is believed to occur in the human situation (*64*).

Evaluation of Cancer Therapy. Cytostatic drugs and radiation therapy are widely used to treat cancer. Apoptosis is one of the main causes of cell death by these treatment types; therefore, anxA5 could be an option for treatment evaluation. It was demonstrated in animal studies that radiolabeled anxA5 is feasible for the evaluation of chemotherapy. Cyclophosphamide-induced apoptosis could be imaged in vivo with ^{99m}Tc-annexin V-117. Blankenberg et al. showed that HYNIC-anxA5 was able to detect PCD after administration of cyclophosphamide in lymphoma-bearing mice (*7*).

Furthermore, ^{99m}Tc-anxA5 can be administered repetitively to tumor-bearing rats without a significant change in the radiopharmaceutical biodistribution. This method may be applicable for tracking tumor shrinkage and other apoptosis-related processes in a rather narrow time frame without affecting imaging quality (*65*).

^{111}In-PEG-anxA5 seems to be suitable as an option to enable long-term imaging of tumors. Recently, the imaging properties of ^{111}In-labeled anxA5 with a long duration of circulation were evaluated in a mouse study. ^{111}In-diethylenetriaminepentaacetic acid-PEG-anxA5 was prepared to meet this goal (*62*). Imaging studies were performed with mice bearing subcutaneously inoculated human mammary tumors. The mice were treated with poly(L-glutamic acid)-paclitaxel, monoclonal antibody C225 (cetuximab), or a combination of poly(L-glutamic acid)-paclitaxel and C225. ^{111}In-Diethylenetriaminepentaacetic acid-PEG-anxA5 showed significantly more uptake in treated tumors than in nontreated tumors, as determined 4 d after cytotoxic therapy (*66*). However, the high uptake of the radiopharmaceutical in the liver and spleen hampered the imaging of targets in the latter region. A similar problem was described for BTAP-anxA5 in humans (*48*).

Fluorescence-labeled anxA5 also was tested for imaging of the tumor response. Petrovsky et al. (*67*) demonstrated that cyclophosphamide treatment of CR8 variants of Lewis lung carcinoma in mice caused a significant increase in the near-infrared fluorescence intensity of Cy5.5-labeled anxA5 in the tumor.

Other Animal Models. Various investigators have shown that HYNIC-anxA5 is able to detect PCD caused by acute transplant rejection of the heart (*7*), lungs (*68*), and liver (*69*) in rats as well as cerebral ischemia in rabbits (*70*). HYNIC-anxA5 imaging showed a 2- to 6-fold increase in the uptake of radiolabeled anxA5 at sites of PCD in the animal models of transplant rejection. Furthermore, immunohistochemical staining of cardiac allografts for anxA5 revealed intense staining of numerous myocytes (*7*). In the model of cerebral ischemia, anxA5 images showed multifocal brain uptake in both hemispheres of experimental animals but not sham-treated control animals. Histologic analysis of the brains from experimental animals demonstrated scattered pyknotic cortical and hippocampal neurons. The absence of positive staining by terminal deoxynucleotidyltransferase-mediated dUTP nick-end labeling (TUNEL) was indicative of a necrosislike cell death pathway (*70*). The occurrence of PCD was demonstrated in an animal model of rheumatoid arthritis (*36*). The amount of PS expression as a determination of the severity of apoptosis in the paws of mice with type II collagen–induced rheumatoid arthritis was shown to be almost 3 times higher than that in the control group.

A significant induction of apoptosis in the spleen was shown in mice that underwent 5-Gy whole-body irradiation. This result was obtained with the TUNEL assay. Moreover, 4-fold more ^{125}I-anxA5 was found in the spleens of treated animals than in control animals (*58*).

PCD imaging in inflammation was further evaluated in an animal model of myocarditis, in which enhanced uptake of radiolabeled anxA5 was shown in the hearts of animals with active myocarditis. This myocarditis was triggered by immunization of rats by infusion of porcine cardiac myosin. The animals formed antibodies against the myosin and subsequently developed myocarditis. Although the imaging in this model was done ex vivo, a correlation was shown between the severity of the myocarditis and the amount of anxA5 uptake (*71*).

In conclusion, both imaging and monitoring of PCD with labeled anxA5 are likely to be feasible in animal models. When the concepts tested in animals can be translated to humans, a more rational use of treatment options will become available.

Biodistribution and Pharmacokinetics of Radiolabeled AnxA5 in Humans

Technetium-Labeled AnxA5. The suitability of 2 types of ^{99m}Tc-anxA5 for in vivo scintigraphy of apoptotic cells was investigated, and the pharmacokinetics and biodistribution of ^{99m}Tc-imino-anxA5 and ^{99m}Tc-BTAP-anxA5 were compared (*43,47,48*). ^{99m}Tc-Imino-anxA5 was administered intravenously to 7 patients and 1 healthy volunteer, and ^{99m}Tc-BTAP-anxA5 was administered to 12 patients. All patients in the pharmacokinetic study had myocardial disease.

The concentration in plasma, excretion, and biodistribution of ^{99m}Tc-anxA5 were measured, as were the levels of anxA5 antigen. The kinetic data for both radiopharmaceuticals in plasma best fitted a 2-compartment model. Both preparations had similar half-lives (about 20 min and 4 h for the first and second compartments, respectively) but had different distributions over the 2 compartments. Levels of anxA5 antigen in plasma showed a broad variation. Both radiopharmaceuticals accumulated in the kidneys, liver, and gut (Fig. 4, 2 left and 2 middle views). BTAP-anxA5 had faster clearance and a lower radiation dose than imino-anxA5. It is obvious from these data that the imaging of apoptosis in the abdomen will be difficult with both radiopharmaceuticals, especially with BTAP-anxA5, because of its faster appearance in the gut (Fig. 4, 2 left and 2 middle views) (*43,48*).

HYNIC-anxA5 was investigated with a similar methodology (*53*). Six healthy male volunteers entered the study. About 250 MBq of HYNIC-anxA5 were injected intravenously. Subsequently, whole-body scans were obtained (Fig. 4, 2 right views). It was shown that the kidneys accumulated approximately 50% of the injected dose at 3 h after injection. Furthermore, the radiopharmaceutical was taken up by the liver, the red marrow, and the spleen. Activity in blood was almost completely cleared with a half-life of about 24 min. The biologic half-life of the radiopharmaceutical was long (approximately 70 h). Excretion of the activity was predominantly through the urine (approximately 23% at 24 h), and hardly any activity was seen in the bowel or feces. The authors concluded that HYNIC-anxA5 is a safe radiopharmaceutical, having a favorable biodistribution, compared with BTAP-anxA5 and imino-anxA5, for the imaging of apoptosis with an acceptable radiation dose (*53*).

Iodine-Labeled AnxA5. The ^{123}I-anxA5 biodistribution in human volunteers was investigated by Lahorte et al. (*59*). They administered the radiopharmaceutical to 6 human volunteers. There seemed to be some initial hampering of imaging because of uptake of the radiopharmaceutical in the stomach and thyroid (*59*). However, at 21 h after administration, rather low overall uptake in most organs was obtained. Theoretically, this finding is promising for the imaging of apoptotic processes in the kidneys, such as transplant rejection. Furthermore, the longer half-life (13 h) of ^{123}I than of ^{99m}Tc enables imaging to be scheduled later after administration. This labeling method still needs more investigation, as no imaging studies have been described yet.

PRESENT: CURRENT CLINICAL NUCLEAR MEDICINE APPLICATIONS

In vivo imaging of cell death is an example of MI. MI is an in vivo method for the characterization and measurement of biologic processes at the molecular level by use of imaging procedures. MI of cell death attempts to visualize one of the key components of homeostasis and disease, that is, the detection of cells performing a cell death program. A summary of all relevant clinical imaging results with anxA5 is shown in Table 2.

Various investigators have used the high affinity of labeled anxA5 for cells expressing PS to detect cell death on a macroscopic level in different types of diseases. Until now, results have been obtained with ^{99m}Tc-anxA5.

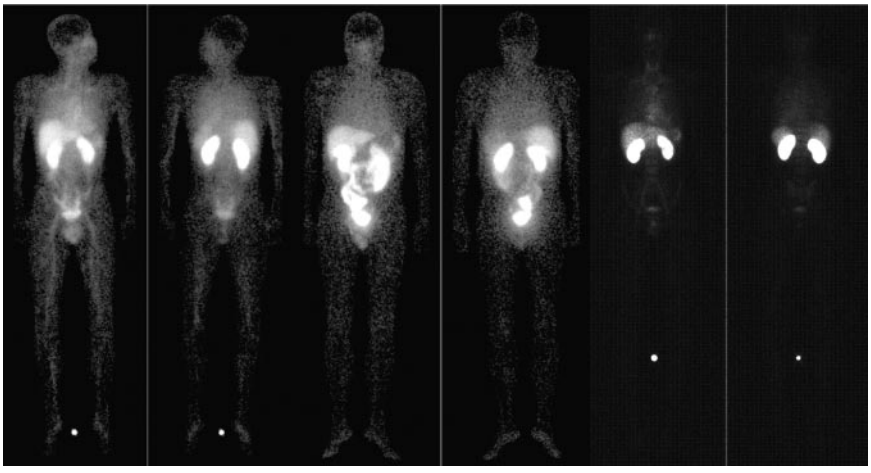

FIGURE 4. Views of whole-body scans of male volunteer (35 y) (2 left views), male patient (53 y) (2 middle views), and male volunteer (22 y) (2 right views) taken after administration of 440 MBq of imino-anxA5, 566 MBq of BTAP-anxA5, and 263 MBq of HYNIC-anxA5, respectively. In each set of views, anterior is on left and posterior is on right. These views demonstrate low uptake of HYNIC-anxA5 in abdomen, compared with that of other 2 isotope conjugation types for anxA5. HYNIC-anxA5, however, shows more uptake in kidneys than either of other conjugation types. Adapted from (*43,53*).

TABLE 2
Summary of Studies of Clinical Imaging

Cell death imaging targets in studies supporting clinical evidence	Reference(s)
Cardiovascular disease	
Myocardial infarction	*2,64*
Cardiac allograft rejection	*39*
Heart failure	*74*
Carotid atherosclerosis	*40*
Oncology	
Intracardiac tumors (malignant: ^{99m}Tc-anxA5 uptake; benign: so far no ^{99m}Tc-anxA5 uptake)	*40,79*
Head and neck tumors	*42*
Non-Hodgkin's lymphoma	*43,85*
Recurrent follicular lymphoma	*86*
Leukemia	*87*
Non–small cell lung cancer	*85*
Sarcoma	*43*
Breast cancer	*43,85*
Cancer therapy: positive correlation between ^{99m}Tc-anxA5 uptake and therapy efficacy	*85,87*

Cell Death in Cardiovascular Disease

An increased occurrence of PCD is common in cardiovascular diseases. Myocardial infarction, heart failure, and atherosclerosis are typical pathologic processes in which apoptosis plays a dominant role. There is a difference between cell death in acute processes, such as myocardial infarction, and the chronic forms of PCD, which are seen in, for example, heart failure. Myocardial infarction is ultimately more likely to cause necrosis rather than apoptosis. This process is caused by intense energy exhaustion from the initial apoptotic cascade, as it is postulated that terminally differentiated cells are very sensitive to adenosine triphosphate depletion. However, when the infarction ischemia is followed by reperfusion, the necrotic pathway is often remodulated into apoptotic cell death (*72*).

Cell death in chronic cardiac disease is not a straightforward process, as apoptosis may occur without the execution phase leading to cell death. Apoptosis occurs in the latter process through cytochrome *c* release and caspase 3 and caspase 8 activation. However, the cell nucleus remains intact and the cell is kept alive. This cellular state is called apoptosis interruptus. These cells may eventually die from necrosis, or they may continue their lives dysfunctionally, like "zombie" myocytes (*72*).

Myocardial Infarction. Clinical studies were performed with patients undergoing myocardial infarction and subsequent reperfusion obtained by percutaneous transluminal coronary angioplasty (*2,64*). Imaging of perfusion (with ^{99m}Tc-sestamibi, ^{99m}Tc-tetrofosmin, or ^{201}Tl) as well as cell death (with ^{99m}Tc-anxA5) was carried out. Under these circumstances, the defect area seen on a perfusion image strongly correlated with the area of increased uptake of ^{99m}Tc-anxA5 (Fig. 5) (*64*). Furthermore, the uptake of ^{99m}Tc-anxA5 in the infarcted area was shown to last up to 4 d after acute myocardial infarction (*64*). These areas of anxA5 uptake in myocardial infarction probably indicate preventable cell loss, as shown in the mouse study of Dumont et al. (*6*) Arguably, "rescued" cardiomyocytes can again regain their function and thereby provide a better outcome after acute myocardial infarction. Whether this is true in the human situation and whether anxA5 can be used as an endpoint to measure cell loss is as yet unknown. Investigations are ongoing in this area.

Cardiac Allograft Rejection. A second application of MI with radiolabeled anxA5 for PCD was first described in 2001 by Narula et al. (*39*). This study focused on cardiac allograft rejection in transplant patients. The diagnosis of rejection of the donor heart poses a difficult clinical prob-

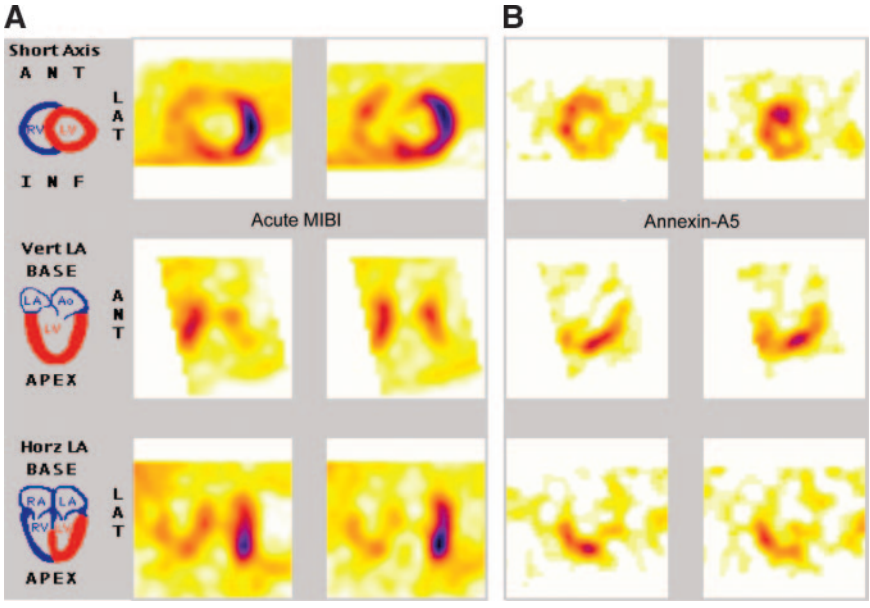

FIGURE 5. (A) Methoxyisobutylisonitrile (MIBI) scintigraphy depicting area of perfusion, indicating area at risk. (B) Binding of ^{99m}Tc-anxA5 to reperfused myocardium, indicative of presence of PCD. ANT = anterior; LAT = lateral; INF = inferior; Vert LA = vertical long axis; Horz LA = horizontal long axis; RV = right ventricle; LV = left ventricle; LA = left atrium; Ao = aorta; RA = right atrium.

lem. Early diagnosis is important because rejection eventually can be influenced by medication that suppresses the inflammatory response to the donor heart. Repeat surgery could be another possible consequence of rejection. The common way to monitor possible rejection of the transplanted heart is to take myocardial biopsies and scan for certain morphologic features. Because these processes have to be monitored over time, multiple biopsies have to be taken, adding to the risk of complications. SPECT with labeled anxA5 for PCD could provide a noninvasive method for identifying patients with cardiac allograft rejection.

In the study of Narula et al. (*39*), all patients ($n = 18$) underwent a ^{99m}Tc-anxA5 SPECT study, and biopsies were taken. When assessing the SPECT images, 2 masked observers were in agreement about the uptake of radiolabeled anxA5 in the myocardium of 5 of these patients. In 3 and 2 cases, focal uptake and general uptake, respectively, of labeled anxA5 were observed in the left ventricle. Tissue sections from the myocardial biopsies were assessed by standard hematoxylin–eosin (H&E) staining, TUNEL staining, and staining for activated caspase 3. H&E staining revealed no or only limited abnormalities in the patients showing no uptake of radiolabeled anxA5. Also, no activation of caspase 3 was observed. In patients showing focal uptake, more severe abnormalities were revealed by H&E staining, when scoring was done according to the recommendations of the International Society of Heart and Lung Transplantation (ISHLT). Scattered cardiomyocytes showed evidence of activation of caspase 3. The 2 patients showing general uptake of labeled anxA5 were scored as having a severe transplant rejection reaction according to ISHLT guidelines and showed many cardiomyocytes with activated caspase 3. TUNEL staining was positive in all but 2 patients.

These data, together with the previously reported data on cardiac allograft rejection in animals, provide proof of the concept for the detection of PCD in patients with cardiac allograft rejection. This method could provide the clinician with an important imaging modality for identifying patients at risk, for monitoring therapy, and for assessing the efficacy of new treatment modalities, such as cell death blockers, in graft rejection (*39,73*).

Heart Failure. Recently, Kietselaer et al. investigated the feasibility of ^{99m}Tc-anxA5 imaging in patients with heart failure (*74*). This disease is defined by a decrease in myocardial functionality, which leads to the upregulation of compensatory mechanisms. These, in turn, cause additional damage to heart function (*75,76*). Functional cell death and loss of heart muscle cell functionality are believed to be important pathologic conditions in heart failure (*77*). Hence, PS expression is very likely to occur; therefore, ^{99m}Tc-anxA5 imaging has been evaluated as a diagnostic tool.

In the study of Kietselaer et al. (*74*), 9 patients with severe congestive heart failure (left ventricular function, <0.35) were investigated. SPECT images from 5 of the 9 patients showed myocardial uptake of ^{99m}Tc-anxA5 (Fig. 6). A recent worsening of the disease strongly correlated with the uptake of ^{99m}Tc-anxA5 in the myocardium, as all ^{99m}Tc-anxA5-negative patients had stable disease and all positive patients had progressive disease. Therefore, it seems likely that ^{99m}Tc-anxA5 imaging is able to discern patients with accelerated myocardial cell loss. This kind of imaging may offer a new option for intervention to be able to prevent the loss of cardiac function (*74*).

Atherosclerosis. Imaging of PS expression also is possible in unstable artherosclerotic regions. Apoptosis was linked previously to atherosclerosis (*78*). It would be clinically important to differentiate stable from unstable

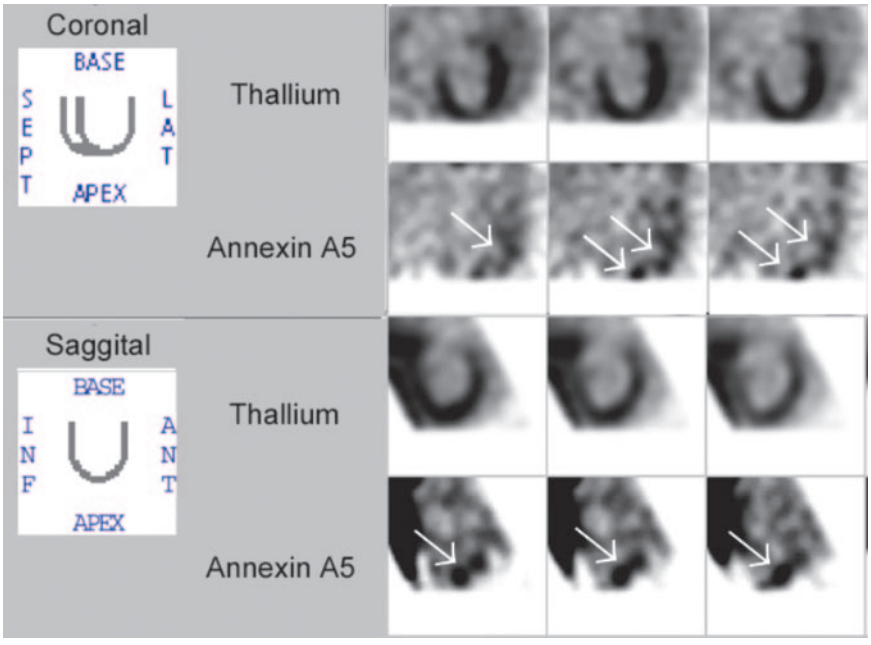

FIGURE 6. Example of ^{99m}Tc-anxA5 uptake in patient with heart failure. Dual-isotope scan shows multifocal anxA5 uptake in patient with idiopathic dilated cardiomyopathy. (Top rows) ^{201}Tl images for orientation purposes. (Bottom rows) Corresponding anxA5 images showing multifocal uptake (arrows). SEPT = septal; LAT = lateral; INF = inferior; ANT = anterior. Adapted from (*74*).

plaques, especially in the carotid artery. Unstable plaques, showing increased apoptosis, could develop thrombosis with subsequent cerebrovascular accidents.

^{99m}Tc-anxA5 imaging in patients with atherosclerotic lesions in the carotid artery therefore could be of value for the noninvasive examination of their apoptotic cell status. In a ^{99m}Tc-anxA5 patient study for the evaluation of artherosclerotic plaques, we imaged 4 patients with a recent or remote history of transient ischemic attack. We performed imaging before removal of the carotid lesions. The images and histologic examination of the artherosclerotic carotid lesions removed from the patients (Fig. 7) revealed that anxA5 uptake in the lesions correlated highly with plaque instability (*40*). This finding was illustrated by ^{99m}Tc-anxA5-negative control samples taken from the same patients. We removed artherosclerotic lesions without evident ^{99m}Tc-anxA5 uptake. Histologic analysis of these lesions showed a stable plaque structure. The conclusion of this pilot study is that imaging of artherosclerotic plaques with ^{99m}Tc-anxA5 may help to identify plaque instability (*40*). Further research involving more patients is ongoing to establish this method.

Tumor Imaging

Homeostasis is disturbed in cancer as well. Tumor development is caused by increased cell proliferation, decreased cell death, or both. In some cancers, cell death is increased, but apparently not sufficiently to prevent the growth of the tumor. ^{99m}Tc-AnxA5 is suitable for imaging of the apoptotic cell status of a tumor.

Intracardiac Tumors. We gained experience in the field of intracardiac tumors during the last few years. Clinical anxA5 imaging of tumors was done in 2 rare cases of endocardial tumors (*41,79*). Endocardial tumors have an incidence of 0.02%–0.3%, and most endocardial tumors, about 70%–90%, are benign (*79–82*). However, they do pose a difficult diagnostic problem for the clinician. "Classic" imaging modalities, such as CT, MRI, and echocardiography, provide excellent data on localization, size, shape, hemodynamic consequences, and pericardial ingrowth of the tumor. These techniques, however, are unable to inform the clinician about the benign or malignant nature of the tumor. Taking a biopsy could aid in making the diagnosis for such tumors, but this procedure carries a very high risk of embolic complications. High proliferation and cell death rates are found in some malignant tumors, such as sarcomas. These properties are in sharp contrast to the pathologic properties of benign tumors. We tested the hypothesis that imaging of these tumors with radiolabeled anxA5 could differentiate between benign and malignant tumors in the heart.

A dual-isotope imaging technique was used for orientation purposes. ^{201}Tl and ^{99m}Tc-anxA5 were infused and imaged simultaneously. The images obtained for both compounds were combined to localize the possible anxA5 uptake within the area of the left ventricle. The first case was a patient presenting with collapse and progressive dyspnea (*41*). The dual-isotope imaging technique showed marked uptake of labeled anxA5 within the area of the tumor (Fig. 8). After surgery, the tumor was placed ex vivo under a γ-camera, which showed increased radioactive uptake. The tumor was found to be an undifferentiated sarcoma (Fig. 9). The binding of anxA5 to the membranes of tumor cells was

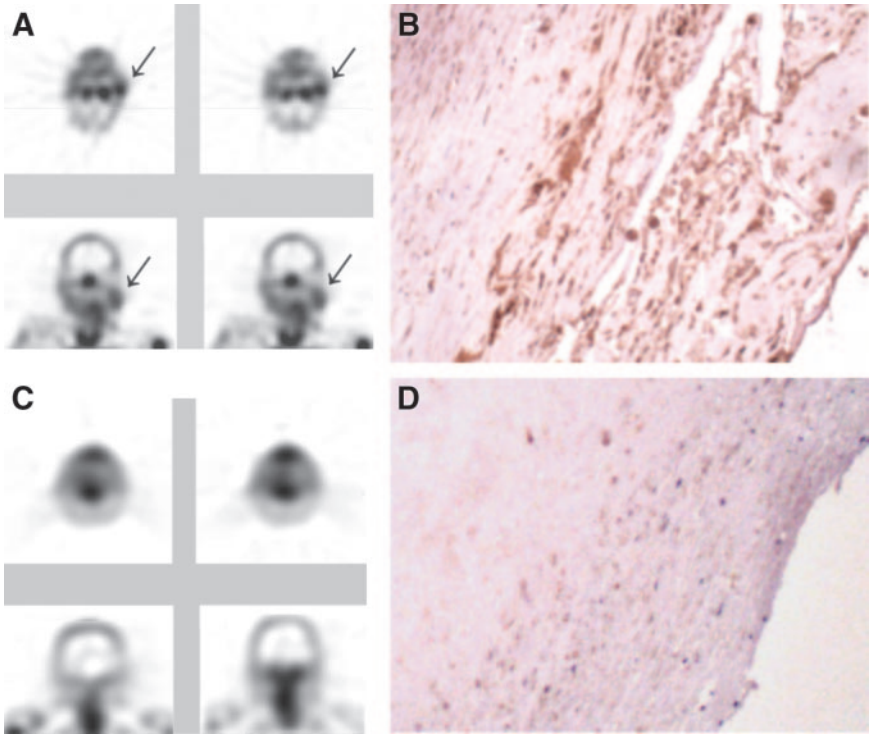

FIGURE 7. ^{99m}Tc-AnxA5 imaging in patients with atherosclerosis. (A) Transverse and coronal SPECT views from patient who had had transient ischemic attack 3 d before imaging. Although stenosis was clinically significant in both carotid arteries, uptake of anxA5 was evident only in culprit lesion (arrows). (B) Histopathologic examination of tissues from this patient shows extensive binding of anxA5 detected by rabbit antiannexin antibodies. (C) For another patient, who had had transient ischemic attack 3 mo before imaging, images do not show any uptake of anxA5. (D) Similarly, histopathologic analysis does not show significant binding of anxA5, although lesion within the carotid artery is evident. Adapted from (*40*).

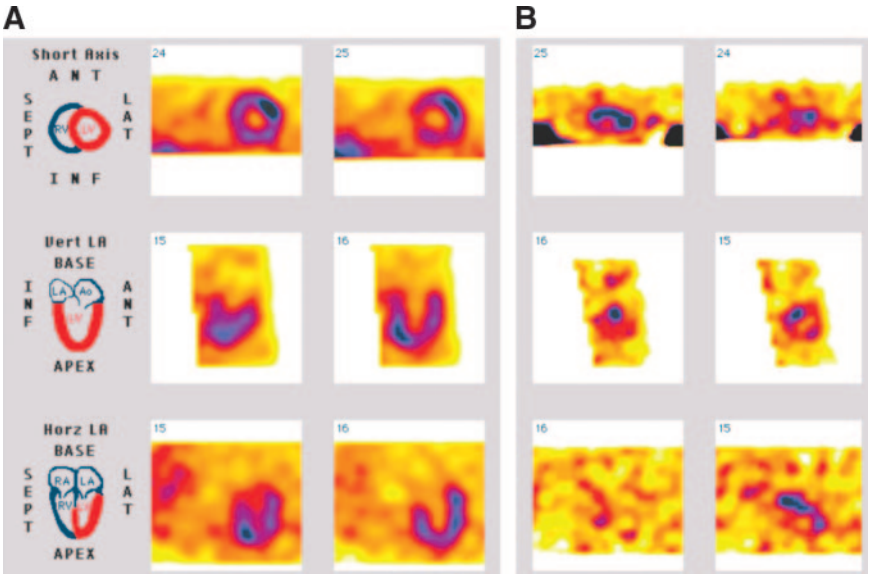

FIGURE 8. (A) Thallium perfusion scintigraphy of malignant tumor showing perfused myocardium of left ventricle in short-axis orientation. (B) Increased uptake of BTAP-anxA5 within contour of left ventricle on short-axis SPECT with orientation similar to that of perfusion scintigram. ANT = anterior; SEPT = septal; LAT = lateral; INF = inferior; Vert LA = vertical long axis; Horz LA = horizontal long axis; RV = right ventricle; LV = left ventricle; LA = left atrium; Ao = aorta; RA = right atrium. Adapted from (*41*).

demonstrated by immunohistochemical means. Furthermore, the presence of activated caspase 3 was detected (Fig. 9) (*41*). This case report provides evidence that PCD is likely to be detected in a malignant tumor by imaging with radiolabeled anxA5.

In the second case, a patient presented with similar symptoms. Again, a dual-isotope imaging technique was used. No uptake of labeled anxA5 within the area of the tumor was demonstrated. The tumor ex vivo also showed hardly any radioactive uptake when placed under a γ-camera. Histologic analysis revealed a myxoma, a benign intracardiac tumor. No anxA5 or activated caspase 3 was detected in the tumor tissue. These data are shown in Figure 10.

Taken together, these data suggest that the anxA5 imaging protocol may be useful for studying the biology of tumors that are difficult to access for biopsies (*79*). There is some discussion about the nature of PS expression within a tumor. Ran et al. (*83*) reported that endothelial cells lining the blood vessels of the tumor vasculature express PS at their surface while alive. Finding that the hypothesis of Ran et al. (*83*) is true would complicate the interpretation of the uptake of anxA5 by tumor cells.

Head and Neck Cancer. van de Wiele et al. (*42*) succeeded in imaging PCD in head and neck cancer. They reported on the relationship between quantitative tumor HYNIC-anxA5 uptake and the number of apoptotic tumor cells derived from histologic analysis. All patients were examined by CT and HYNIC-anxA5 SPECT and then underwent surgical resection of the suspected primary or recurrent tumor. Quantitative tumor HYNIC-anxA5 uptake correlated well with the number of apoptotic cells determined by TUNEL staining, when only tumor samples with no or minimal amounts of necrosis were considered (*42*).

Other Tumor Types. We were able to image PCD in patients with lymphoma, sarcoma, and non–small cell lung carcinoma (an example of the latter is shown in Fig. 11) (*43*). The sarcoma image shows that a large necrotic central area within the tumor can be present. Figure 12 shows a planar image at 16 h after injection of ^{99m}Tc-anxA5. Increased uptake of ^{99m}Tc-anxA5 in the right upper leg of the patient with sarcoma suggests PS expression in this region. The latter is best seen in the anterior image. The central region without activity corresponds to an area of necrosis on a CT scan (*43*).

Cancer Treatment Efficacy Evaluation with ^{99m}Tc-AnxA5. Imaging of tumors with ^{99m}Tc-anxA5 in theory has even more applications than imaging with ^{99m}Tc-anxA5 for cardiac disease because of the possibility of evaluating the apoptotic cell status of a tumor before and after therapy. The animal work of Mochizuki et al. (*84*) showed that the effectiveness of chemotherapy can be evaluated after a single dose of chemotherapy. At present there is some evidence that the same principle can be applied in clinical medicine. This evidence should be sustained by large clinical trials. If so, this technique would be an extremely valuable addition to conventional imaging. The application of ^{99m}Tc-anxA5-guided cytotoxic therapy might enhance individualized therapy, influence clinical decision making, and aid in the timing of surgery. Overall patient survival and quality of life could be further improved.

Belhocine et al. (*85*) showed that responders who had a positive ^{99m}Tc-anxA5 scan after chemotherapy had better survival rates than those who did not. No tracer uptake was observed before treatment in all cases. Seven patients showed ^{99m}Tc-anxA5 uptake at tumor sites 24–48 h after the first course of chemotherapy. These patients had either a complete response ($n = 4$) or a partial response ($n = 3$). Furthermore, 6 of the 8 patients who showed no significant posttreatment tumor uptake of ^{99m}Tc-anxA5 had progressive disease. Two patients with breast cancer had a partial response, despite the lack of tracer uptake after treatment.

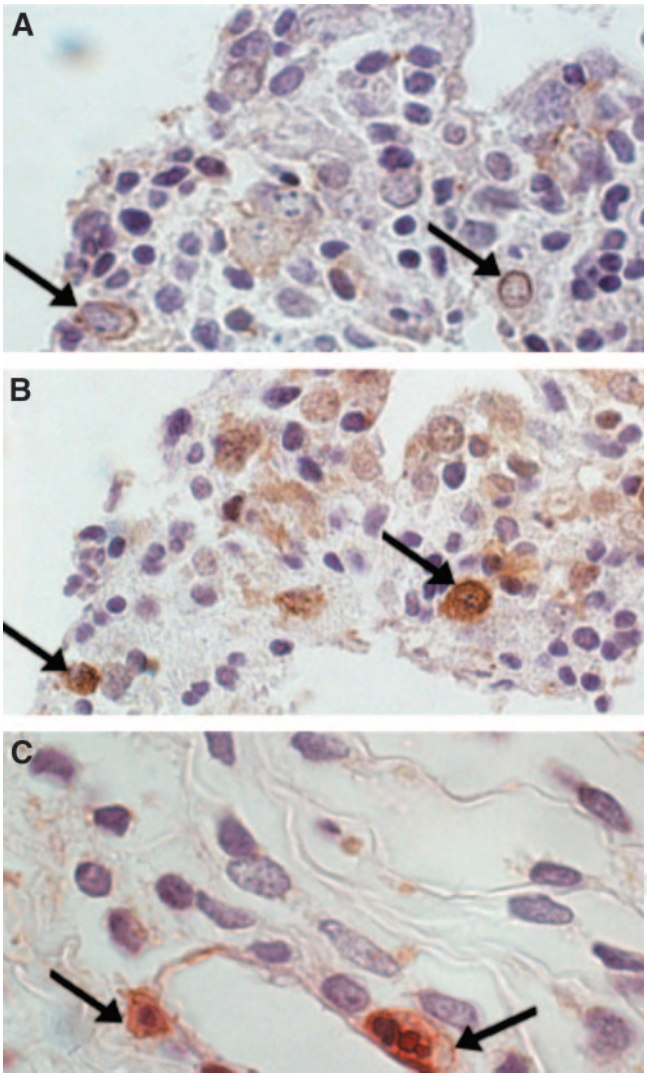

FIGURE 9. Malignant intracardiac sarcoma (immunohistologic analysis). (A) AnxA5 antibody staining (brown staining, arrows). (B) CM-1 antibody staining, indicating caspase 3 activation (brown staining, arrows). (C) Double staining with both CM-1 antibody (red staining) and anxA5 antibody (brown staining, arrows). Adapted from (*41*).

Overall survival and progression-free survival were related to tracer uptake in treated lung cancers and lymphomas (*85*).

Recently, Haas et al. (*86*) showed that the principle of therapy evaluation also can be applied for HYNIC-anxA5 in patients undergoing radiotherapy (*86*). ^{99m}Tc-AnxA5 imaging was performed for 11 patients with recurrent follicular lymphoma. Scintigraphy was done before and 24 h after the last fraction of the 2 × 2 Gy involved field radiotherapy regimen. Cytologic analysis was performed to determine the optimal time window for apoptosis detection and to confirm the apoptotic nature of the response. Scintigraphy with ^{99m}Tc-anxA5 (total-body studies and SPECT of the irradiated sites) was performed at 4 h after injection. Tumor ^{99m}Tc-AnxA5 uptake was scored in a semiquantitative manner. Response evaluation was performed after 1 and 4 wk in terms of both completeness and speed of remission. ^{99m}Tc-AnxA5 uptake at baseline was absent in 6 patients and weak in 5 patients. The optimal time period for apoptosis assessment was determined by sequential cytologic analyses to be between 24 and 48 h after the last fraction of the 2 × 2 Gy regimen. Baseline cytologic analysis correlated with baseline ^{99m}Tc-anxA5 uptake in all patients. ^{99m}Tc-AnxA5 uptake matched posttreatment cytologic analysis in all but 1 patient. In these 10 patients, cytologic analysis and ^{99m}Tc-anxA5 uptake correlated well with the clinical response. Therefore, the authors concluded that tumor ^{99m}Tc-anxA5 uptake is likely to increase after 2 × 2 Gy involved field radiotherapy. Hence, apoptotic cell death can be observed on day 4 of this regimen and, if observed, predicts complete remission within 1 wk (*86*).

Furthermore, Kartachova et al. were able to identify tumor ^{99m}Tc-anxA5 uptake and relate it to treatment response (*87*). This study was performed for patients with malignant lymphoma, leukemia, non–small cell lung carcinoma, and head and neck squamous cell carcinoma. Changes in tumor ^{99m}Tc-anxA5 uptake and clinical response were shown to be statistically significant. Complete or partial tumor response was correlated with a marked increase in ^{99m}Tc-anxA5 accumulation during early treatment over the baseline value. Also, pretreatment scans demonstrated predominantly low tumor ^{99m}Tc-anxA5 uptake and no significant increase early after treatment in cases of stable or progressive disease (*87*).

Cancer is interesting in terms of both tumor imaging and therapy evaluation with radiolabeled anxA5. However, much information on exact times for tumor therapy and tumor imaging is still needed. The latter are likely to depend on the tumor characteristics as well as the kind of cytotoxic therapy used.

Clinical Impact of Cell Death Imaging

The current understanding of the role of PCD in pathogenesis and therapeutic regimens implies a significant clinical value for the anxA5 imaging protocol. Its potential significance in patient management has been underscored by preclinical studies and initial patient studies. These studies have shown that the anxA5 imaging protocol may provide clinically relevant information about the biology of lesions and about the efficacy of therapeutic treatments.

First, the imaging protocol may discern between stable and unstable atherosclerotic lesions (*40*), as discussed earlier in this review. This promise arises from preclinical and preliminary clinical studies. In the latter case, the promise needs to be substantiated by a clinical study with a larger patient population. Finding that the proposition is true would have a great impact on the management of patients with atherosclerotic plaques in carotid and coronary arteries.

Another application that may have a clinical impact related to retrieving biologic information from a lesion concerns the diagnosis of patients with tumors that are not

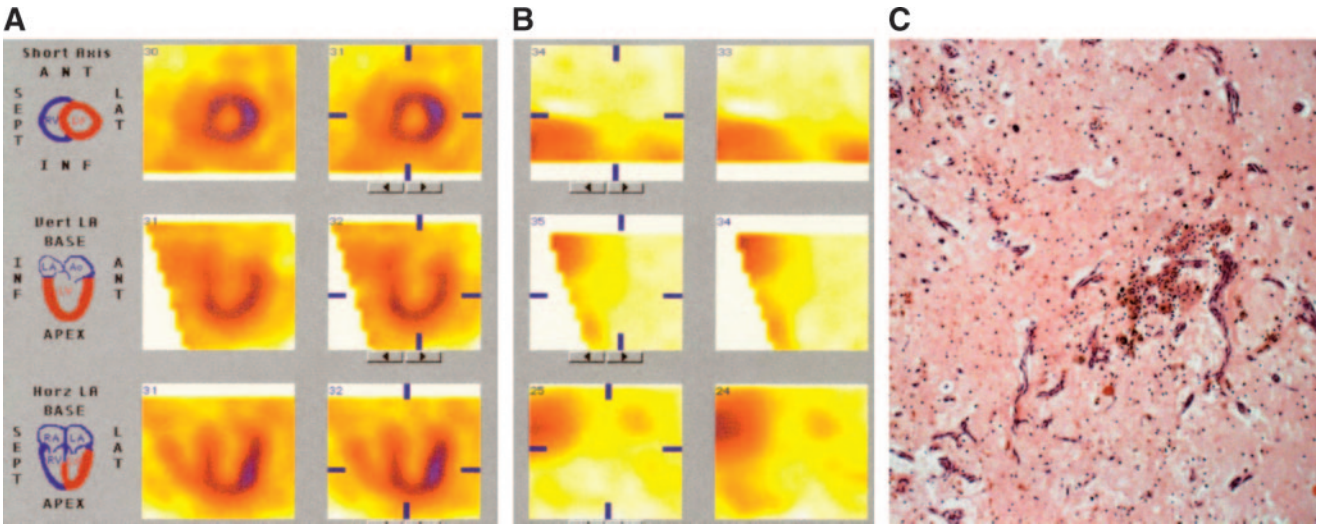

FIGURE 10. (A) Thallium perfusion scintigraphy of benign tumor shows perfused left ventricle of myocardium in short-axis orientation. (B) No increased uptake of BTAP-anxA5 can be seen within contour of left ventricle on short-axis SPECT with orientation similar to that of perfusion scintigram. (C) Upon histologic examination, tissue was found to have features of myxoma, with clustering of nuclei and large cellular matrices. No significant anxA5 antibody uptake and no caspase 3 activation could be demonstrated. ANT = anterior; SEPT = septal; LAT = lateral; INF = inferior; Vert LA = vertical long axis; Horz LA = horizontal long axis; RV = right ventricle; LV = left ventricle; LA = left atrium; Ao = aorta; RA = right atrium.

accessible for biopsies, such as cardiac tumors (*41,79*) There is some evidence that highly malignant tumors have a high apoptotic index. The first results obtained with the anxA5 imaging protocol are promising (*79*). More clinical studies are required to validate this application.

Second, the anxA5 imaging protocol may help to assess therapeutic efficacy early after the start of therapy. This application has been suggested from clinical studies in which cancer patients underwent the anxA5 imaging protocol before and after the beginning of radiotherapy (*87*) and chemotherapy (*85*). This promise encompasses the possibility of determining rapidly the success of a specific treatment for an individual undergoing anticancer therapy.

Taken together, data indicate that the anxA5 imaging protocol bears the promise to make personalized medicine possible for cardiovascular and oncologic cases.

FUTURE

We believe that the possibilities for the application of anxA5 in diagnostic techniques, treatment evaluation, and therapy approaches in the future are broad. The following

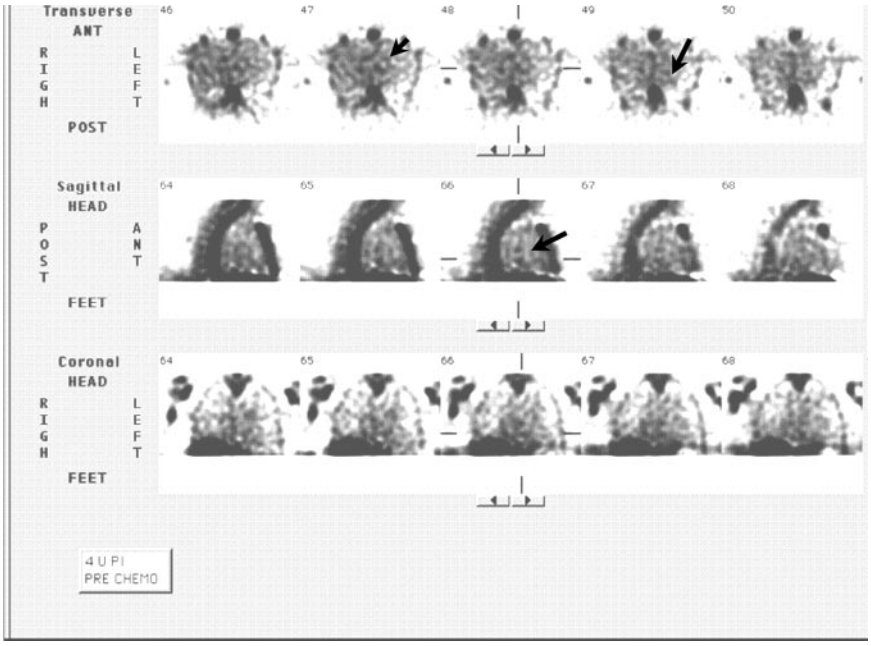

FIGURE 11. SPECT image of non–small cell lung carcinoma. Increased uptake of HYNIC-anxA5 can be seen within thorax (arrows). ANT = anterior; POST = posterior; 4 h PI = 4 h after injection of HYNIC-anxA5; PRE CHEMO = before chemotherapy.

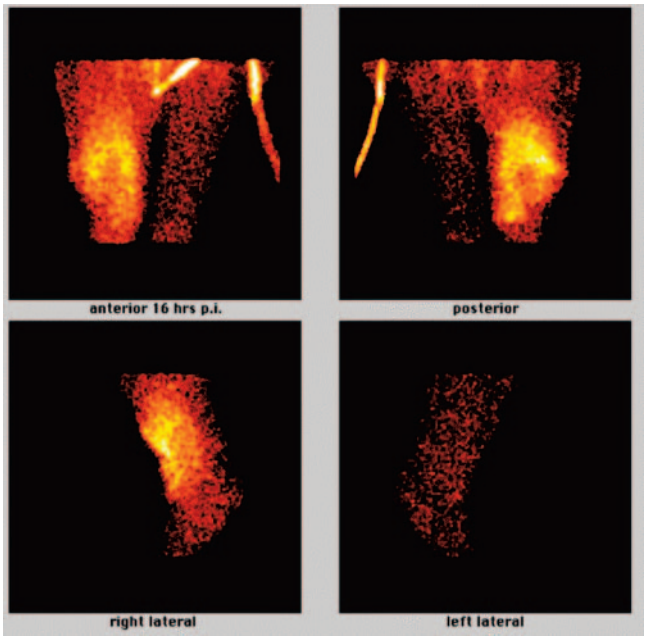

FIGURE 12. Planar images of patient with sarcoma of right leg at 16 h after injection (p.i.) of BTAP-anxA5. There was increased uptake of BTAP-anxA5 in major part of upper right leg, with central zone of decreased activity. Almost no uptake was seen in left leg. Adapted from (*43*).

requirements need to be met to ensure further development of anxA5 as a diagnostic and therapeutic tool:

- The development for human use of new PET anxA5 probes to enhance the resolution of images should be pursued. Good candidates are ^{68}Ga-anxA5 and ^{18}F-anxA5 conjugates (*45*). Because ^{68}Ga is not expensive and is available through a generator, the cyclotron-produced ^{18}F may be not as practical as ^{68}Ga.

- At this time, there is no sponsored clinical trial program to gain additional information on therapy evaluation with radiolabeled anxA5. Such protocols are a requirement for the further development of anxA5.

- The biodistribution profile for radiolabeled anxA5 is not optimal; therefore, the development of conjugates with a better biodistribution profile should be pursued. The high uptake in liver and kidneys of technetium-labeled anxA5 is a special challenge to the improvement of imaging. As suggested by Tait et al. (*56*), the use of endogenous chelation sites for ^{99m}Tc labeling shows promise in this respect. They lead to better target-to-background ratios and lower uptake in the liver, kidneys, and spleen. ^{123}I-AnxA5 also shows lower uptake in these organs. However, its rather complex labeling method is expected to hamper further clinical development (*59*). The biodistribution of anxA5 imaging tracers was discussed extensively earlier in this article.

- Little is known about the necessary time frame between the administration of radiolabeled anxA5 and subsequent imaging. We assume that this lack of knowledge is caused by coincidence of the biodistribution of the radiopharmaceutical used with the targeted cell death process. For instance, our imaging results with BTAP-anxA5 showed that it is able to visualize a breast tumor at 4 h after administration, whereas acute myocardial infarction can be imaged at 15 h after the administration of BTAP-anxA5 (*43*). With HYNIC-anxA5, however, acute myocardial infarction can be imaged best at 4–6 h after administration of the compound (Leonard Hofstra, unpublished data, November 2003).

- To be able to perform therapy evaluation with anxA5, more information is needed to validate the use of anxA5 for apoptotic or antiapoptotic treatment of disease in humans. The latter would be of great interest for the prediction of treatment outcome in patients. For instance, the use of anxA5 to determine the efficacy of chemotherapy or radiation therapy in cancer to be able to predict patient survival would be of great value. Large clinical trials should be conducted to prove the feasibility of these methods.

- The development of anxA5-containing pharmaceuticals for the targeting of drug treatment in diseases such as cancer would enhance specific treatment of the diseases. Targeted therapy presumably increases treatment efficacy and similarly decreases the probability of adverse reactions in patients. The property of anxA5 to internalize within a cell is certainly of interest with regard to treatment options. The ability of the anxA5 molecule to serve as a carrier for therapeutic agents is a subject for further research.

- Simultaneous measurement of cell proliferation, cell death, and cellular oxygen consumption by use of radiopharmaceuticals labeled with different radionuclides is the ultimate goal of radiotherapists to individualize patient treatment. Nuclear medicine could play an important role in this fascinating approach.

CONCLUSION

AnxA5 was shown to exert various biologic effects in vitro. The ability of anxA5 to bind to PS specifically in the presence of calcium is widely used to detect apoptosis. Hence, anxA5-containing radiopharmaceuticals are an interesting development within the field of nuclear medicine. They have demonstrated the ability to visualize PS expression in various diseases, such as cancer and myocardial infarction. Until now, most experience has been gained with technetium-labeled anxA5. The disadvantage of most conjugation methods for this radioisotope and anxA5 is poor biodistribution. So far, the best candidate for SPECT with

technetium is HYNIC-anxA5. However, other agents also are promising. The use of anxA5 can be further extended by the discovery of new pharmaceuticals that can target apoptotic cells more specifically with anxA5.

REFERENCES

1. Chen M, He H, Zhan S, et al. Bid is cleaved by calpain to an active fragment in vitro and during myocardial ischemia/reperfusion. *J Biol Chem*. 2001;276:30724–30728.
2. Hofstra L, Liem IH, Dumont EA, et al. Visualisation of cell death in vivo in patients with acute myocardial infarction. *Lancet*. 2000;356:209–212.
3. Kolodgie FD, Narula J, Guillo P, Virmani R. Apoptosis in human atherosclerotic plaques. *Apoptosis*. 1999;4:5–10.
4. Leist M, Jaattela M. Four deaths and a funeral: from caspases to alternative mechanisms. *Nat Rev Mol Cell Biol*. 2001;2:589–598.
5. Dumont EA, Reutelingsperger CP, Smits JF, et al. Real-time imaging of apoptotic cell-membrane changes at the single-cell level in the beating murine heart. *Nat Med*. 2001;7:1352–1355.
6. Dumont EA, Hofstra L, van Heerde WL, et al. Cardiomyocyte death induced by myocardial ischemia and reperfusion: measurement with recombinant human annexin-V in a mouse model. *Circulation*. 2000;102:1564–1568.
7. Blankenberg FG, Katsikis PD, Tait JF, et al. In vivo detection and imaging of phosphatidylserine expression during programmed cell death. *Proc Natl Acad Sci U S A*. 1998;95:6349–6354.
8. Koopman G, Reutelingsperger CP, Kuijten GA, et al. Annexin V for flow cytometric detection of phosphatidylserine expression on B cells undergoing apoptosis. *Blood*. 1994;84:1415–1420.
9. Gerke V, Moss SE. Annexins: from structure to function. *Physiol Rev*. 2002;82:331–371.
10. Bohn H, Kraus W. Isolation and characterization of a new placenta specific protein (PP10) [in German]. *Arch Gynecol*. 1979;227:125–134.
11. Reutelingsperger CP, Hornstra G, Hemker HC. Isolation and partial purification of a novel anticoagulant from arteries of human umbilical cord. *Eur J Biochem*. 1985;151:625–629.
12. Reutelingsperger CP, Kop JM, Hornstra G, Hemker HC. Purification and characterization of a novel protein from bovine aorta that inhibits coagulation: inhibition of the phospholipid-dependent factor-Xa-catalyzed prothrombin activation, through a high-affinity binding of the anticoagulant to the phospholipids. *Eur J Biochem*. 1988;173:171–178.
13. Reutelingsperger CP. Annexins: key regulators of haemostasis, thrombosis, and apoptosis. *Thromb Haemostasis*. 2001;86:413–419.
14. Hayes MJ, Moss SE. Annexins and disease. *Biochem Biophys Res Commun*. 2004;322:1166–1170.
15. Hayes MJ, Rescher U, Gerke V, Moss SE. Annexin-actin interactions. *Traffic*. 2004;5:571–576.
16. Moss SE, Morgan RO. The annexins. *Genome Biol*. 2004;5:219.
17. Maurer-Fogy I, Reutelingsperger CP, Pieters J, et al. Cloning and expression of cDNA for human vascular anticoagulant, a Ca2+-dependent phospholipid-binding protein. *Eur J Biochem*. 1988;174:585–592.
18. Kaplan R, Jaye M, Burgess WH, Schlaepfer DD, Haigler HT. Cloning and expression of cDNA for human endonexin II, a Ca2+ and phospholipid binding protein. *J Biol Chem*. 1988;263:8037–8043.
19. Iwasaki A, Suda M, Nakao H, et al. Structure and expression of cDNA for an inhibitor of blood coagulation isolated from human placenta: a new lipocortin-like protein. *J Biochem (Tokyo)*. 1987;102:1261–1273.
20. Blankenberg FG, Strauss HW. Will imaging of apoptosis play a role in clinical care? A tale of mice and men. *Apoptosis*. 2001;6:117–123.
21. Fadok V, Voelker DR, Campbell PA, et al. Exposure of phosphatidylserine on the surface of apoptotic lymphocytes triggers specific recognition and removal by macrophages. *J Immunol*. 1992;148:2207–2216.
22. Zwaal RF, Schroit AJ. Pathophysiologic implications of membrane phospholipid asymmetry in blood cells. *Blood*. 1997;89:1121–1132.
23. Martin SJ, Reutelingsperger CP, McGahon AJ, et al. Early redistribution of plasma membrane phosphatidylserine is a general feature of apoptosis regardless of the initiating stimulus: inhibition by overexpression of Bcl-2 and Abl. *J Exp Med*. 1995;182:1545–1556.
24. Vermes I, Haanen C, Steffens-Nakken H, Reutelingsperger C. A novel assay for apoptosis: flow cytometric detection of phosphatidylserine expression on early apoptotic cells using fluorescein labelled annexin V. *J Immunol Methods*. 1995;184:39–51.
25. Homburg CH, de Haas M, von dem Borne AE, et al. Human neutrophils lose their surface Fc gamma RIII and acquire annexin V binding sites during apoptosis in vitro. *Blood*. 1995;85:532–540.
26. Kroemer G, Martin SJ. Caspase-independent cell death. *Nat Med*. 2005;11:725–730.
27. Fadok VA, Henson PM. Apoptosis: giving phosphatidylserine recognition an assist—with a twist. *Curr Biol*. 2003;13:R655–R657.
28. McLaughlin R, Kelly CJ, Kay E, Bouchier-Hayes D. The role of apoptotic cell death in cardiovascular disease. *Ir J Med Sci*. 2001;170:132–140.
29. Fischer U, Schulze-Osthoff K. Apoptosis-based therapies and drug targets. *Cell Death Differ*. 2005;57:187–215.
30. Green DR, Kroemer G. The pathophysiology of mitochondrial cell death. *Science*. 2004;305:626–629.
31. Zimmermann KC, Bonzon C, Green DR. The machinery of programmed cell death. *Pharmacol Ther*. 2001;92:57–70.
32. Zimmermann KC, Green DR. How cells die: apoptosis pathways. *J Allergy Clin Immunol*. 2001;108(suppl):S99–S103.
33. van Engeland M, Kuijpers HJ, Ramaekers FC, Reutelingsperger CP, Schutte B. Plasma membrane alterations and cytoskeletal changes in apoptosis. *Exp Cell Res*. 1997;235:421–430.
34. Kenis H, van Genderen H, Bennaghmouch A, et al. Cell surface-expressed phosphatidylserine and annexin A5 open a novel portal of cell entry. *J Biol Chem*. 2004;279:52623–52629.
35. Vriens PW, Blankenberg FG, Stoot JH, et al. The use of technetium Tc 99m annexin V for in vivo imaging of apoptosis during cardiac allograft rejection. *J Thorac Cardiovasc Surg*. 1998;116:844–853.
36. Post AM, Katsikis PD, Tait JF, et al. Imaging cell death with radiolabeled annexin V in an experimental model of rheumatoid arthritis. *J Nucl Med*. 2002;43:1359–1365.
37. Glaser M, Collingridge DR, Aboagye EO, et al. Iodine-124 labelled annexin-V as a potential radiotracer to study apoptosis using positron emission tomography. *Appl Radiat Isot*. 2003;58:55–62.
38. Murakami Y, Takamatsu H, Taki J, et al. ^{18}F-Labelled annexin V: a PET tracer for apoptosis imaging. *Eur J Nucl Med Mol Imaging*. 2004;31:469–474.
39. Narula J, Acio ER, Narula N, et al. Annexin-V imaging for noninvasive detection of cardiac allograft rejection. *Nat Med*. 2001;7:1347–1352.
40. Kietselaer BL, Reutelingsperger CP, Heidendal GA, et al. Noninvasive detection of plaque instability with use of radiolabeled annexin A5 in patients with carotid-artery atherosclerosis. *N Engl J Med*. 2004;350:1472–1473.
41. Hofstra L, Dumont EA, Thimister PW, et al. In vivo detection of apoptosis in an intracardiac tumor. *JAMA*. 2001;285:1841–1842.
42. van de Wiele C, Lahorte C, Vermeersch H, et al. Quantitative tumor apoptosis imaging using technetium-99m-HYNIC annexin V single photon emission computed tomography. *J Clin Oncol*. 2003;21:3483–3487.
43. Boersma HH, Liem IH, Kemerink GJ, et al. Comparison between human pharmacokinetics and imaging properties of two conjugation methods for ^{99m}Tc-annexin A5. *Br J Radiol*. 2003;76:553–560.
44. Verbruggen A. Bifunctional chelators for technetium-99m. In: Mather SJ, ed. *Current Directions in Radiopharmaceutical Research and Development*. Dordrecht, The Netherlands: Kluwer Academic Publishers; 1996:31–46.
45. Lahorte CM, Vanderheyden JL, Steinmetz N, et al. Apoptosis-detecting radioligands: current state of the art and future perspectives. *Eur J Nucl Med Mol Imaging*. 2004;31:887–919.
46. Goedemans W, Panek KJ, Ensing GJ, de Jong MTM. A new simple method for labelling of proteins with ^{99m}Tc by derivatization with 1-imino-4-mercaptobutyl groups. In: Nicolini M, Bandolini G, Mazzi U, eds. *Technetium and Rhenium in Chemistry and Nuclear Medicine*. Vol 3. Verona, Italy: Cortina International; 1990:595–604.
47. Kemerink GJ, Liem IH, Hofstra L, et al. Patient dosimetry of intravenously administered ^{99m}Tc-annexin V. *J Nucl Med*. 2001;42:382–387.
48. Kemerink GJ, Boersma HH, Thimister PW, et al. Biodistribution and dosimetry of ^{99m}Tc-BTAP-annexin-V in humans. *Eur J Nucl Med*. 2001;28:1373–1378.
49. Stratton JR, Dewhurst TA, Kasina S, et al. Selective uptake of radiolabeled annexin V on acute porcine left atrial thrombi. *Circulation*. 1995;92:3113–3121.
50. Kasina S, Rao TN, Srinivasan A, et al. Development and biologic evaluation of a kit for preformed chelate technetium-99m radiolabeling of an antibody Fab fragment using a diamide dimercaptide chelating agent. *J Nucl Med*. 1991;32:1445–1451.
51. Yang DJ, Azhdarinia A, Wu P, et al. In vivo and in vitro measurement of apoptosis in breast cancer cells using ^{99m}Tc-EC-annexin V. *Cancer Biother Radiopharm*. 2001;16:73–83.
52. Boersma HH, Stolk LM, Kenis H, et al. The ApoCorrect assay: a novel, rapid method to determine the biological functionality of radiolabeled and fluorescent annexin A5. *Anal Biochem*. 2004;327:126–134.
53. Kemerink GJ, Liu X, Kieffer D, et al. Safety, biodistribution, and dosimetry of

^{99m}Tc-HYNIC-annexin V, a novel human recombinant annexin V for human application. *J Nucl Med*. 2003;44:947–952.
54. Tait JF, Brown DS, Gibson DF, Blankenberg FG, Strauss HW. Development and characterization of annexin V mutants with endogenous chelation sites for (99m)Tc. *Bioconjug Chem*. 2000;11:918–925.
55. Tait JF, Smith C, Gibson DF. Development of annexin V mutants suitable for labeling with Tc(i)-carbonyl complex. *Bioconjug Chem*. 2002;13:1119–1123.
56. Tait JF, Smith C, Blankenberg FG. Structural requirements for in vivo detection of cell death with ^{99m}Tc-annexin V. *J Nucl Med*. 2005;46:807–815.
57. Tait JF, Cerqueira MD, Dewhurst TA, et al. Evaluation of annexin V as a platelet-directed thrombus targeting agent. *Thromb Res*. 1994;75:491–501.
58. Russell J, O'Donoghue JA, Finn R, et al. Iodination of annexin V for imaging apoptosis. *J Nucl Med*. 2002;43:671–677.
59. Lahorte CM, van de Wiele C, Bacher K, et al. Biodistribution and dosimetry study of ^{123}I-rh-annexin V in mice and humans. *Nucl Med Commun*. 2003;24:871–880.
60. Lahorte C, Slegers G, Philippe J, Van de Wiele C, Dierckx RA. Synthesis and in vitro evaluation of ^{123}I-labelled human recombinant annexin V. *Biomol Eng*. 2001;17:51–53.
61. Zijlstra S, Gunawan J, Burchert W. Synthesis and evaluation of a ^{18}F-labelled recombinant annexin-V derivative, for identification and quantification of apoptotic cells with PET. *Appl Radiat Isot*. 2003;58:201–207.
62. Wen X, Wu QP, Ke S, et al. Improved radiolabeling of PEGylated protein: PEGylated annexin V for noninvasive imaging of tumor apoptosis. *Cancer Biother Radiopharm*. 2003;18:819–827.
63. Taki J, Higuchi T, Kawashima A, et al. Detection of cardiomyocyte death in a rat model of ischemia and reperfusion using ^{99m}Tc-labeled annexin V. *J Nucl Med*. 2004;45:1536–1541.
64. Thimister PW, Hofstra L, Liem IH, et al. In vivo detection of cell death in the area at risk in acute myocardial infarction. *J Nucl Med*. 2003;44:391–396.
65. Kuge Y, Sato M, Zhao S, et al. Feasibility of ^{99m}Tc-annexin V for repetitive detection of apoptotic tumor response to chemotherapy: an experimental study using a rat tumor model. *J Nucl Med*. 2004;45:309–312.
66. Ke S, Wen X, Wu QP, et al. Imaging taxane-induced tumor apoptosis using PEGylated, ^{111}In-labeled annexin V. *J Nucl Med*. 2004;45:108–115.
67. Petrovsky A, Schellenberger E, Josephson L, Weissleder R, Bogdanov A Jr. Near-infrared fluorescent imaging of tumor apoptosis. *Cancer Res*. 2003;63:1936–1942.
68. Blankenberg FG, Robbins RC, Stoot JH, et al. Radionuclide imaging of acute lung transplant rejection with annexin V. *Chest*. 2000;117:834–840.
69. Ogura Y, Krams SM, Martinez OM, et al. Radiolabeled annexin V imaging: diagnosis of allograft rejection in an experimental rodent model of liver transplantation. *Radiology*. 2000;214:795–800.
70. D'Arceuil H, Rhine W, de Crespigny A, et al. ^{99m}Tc annexin V imaging of neonatal hypoxic brain injury. *Stroke*. 2000;31:2692–2700.
71. Tokita N, Hasegawa S, Maruyama K, et al. ^{99m}Tc-Hynic-annexin V imaging to evaluate inflammation and apoptosis in rats with autoimmune myocarditis. *Eur J Nucl Med Mol Imaging*. 2003;30:232–238.
72. Narula J, Zaret BL. Noninvasive detection of cell death: from tracking epitaphs to counting coffins. *J Nucl Cardiol*. 2002;9:554–560.
73. Kown MH, Strauss HW, Blankenberg FG, et al. In vivo imaging of acute cardiac rejection in human patients using (99m)technetium labeled annexin V. *Am J Transplant*. 2001;1:270–277.
74. Kietselaer BL, Narula J, Heidendal GA, et al. Noninvasive detection of apoptosis during worsening of human dilated cardiomyopathy using ^{99m}technetium-labelled annexin A5 [abstract]. *Circulation*. 2004;110:436.
75. Zhang J, McDonald KM. Bioenergetic consequences of left ventricular remodeling. *Circulation*. 1995;92:1011–1019.
76. Gomez AM, Valdivia HH, Cheng H, et al. Defective excitation-contraction coupling in experimental cardiac hypertrophy and heart failure. *Science*. 1997;276:800–806.
77. Haider N, Narula N, Narula J. Apoptosis in heart failure represents programmed cell survival, not death, of cardiomyocytes and likelihood of reverse remodeling. *J Card Fail*. 2002;8(suppl):S512–S517.
78. Kolodgie FD, Narula J, Burke AP, et al. Localization of apoptotic macrophages at the site of plaque rupture in sudden coronary death. *Am J Pathol*. 2000;157:1259–1268.
79. Kietselaer B, Thimister PWL, Reutelingsperger CPM, et al. Molecular imaging of cell death in intra-cardiac tumors: a new approach to differential diagnosis in cardiac tumors. *Netherlands Heart J*. 2002;10:312–316.
80. Reynen K. Frequency of primary tumors of the heart [editorial]. *Am J Cardiol*. 1996;77:107.
81. Blondeau P. Primary cardiac tumors: French studies of 533 cases. *Thorac Cardiovasc Surg*. 1990;38(suppl 2):192–195.
82. McAllister HA. Tumors of the cardiovascular system. In: Hartman WH, ed. *Atlas of Tumor Pathology*. Second series ed. Washington, DC: Armed Forces Institute of Pathology; 1978:20–25.
83. Ran S, Downes A, Thorpe PE. Increased exposure of anionic phospholipids on the surface of tumor blood vessels. *Cancer Res*. 2002;62:6132–6140.
84. Mochizuki T, Kuge Y, Zhao S, et al. Detection of apoptotic tumor response in vivo after a single dose of chemotherapy with ^{99m}Tc-annexin V. *J Nucl Med*. 2003;44:92–97.
85. Belhocine T, Steinmetz N, Hustinx R, et al. Increased uptake of the apoptosis-imaging agent (99m)Tc recombinant human annexin V in human tumors after one course of chemotherapy as a predictor of tumor response and patient prognosis. *Clin Cancer Res*. 2002;8:2766–2774.
86. Haas RL, de Jong D, Valdes Olmos RA, et al. In vivo imaging of radiation-induced apoptosis in follicular lymphoma patients. *Int J Radiat Oncol Biol Phys*. 2004;59:782–787.
87. Kartachova M, Haas RL, Valdes Olmos RA, et al. In vivo imaging of apoptosis by ^{99m}Tc-annexin V scintigraphy: visual analysis in relation to treatment response. *Radiother Oncol*. 2004;72:333–339.

JNM The Journal of NUCLEAR MEDICINE

Past, Present, and Future of Annexin A5: From Protein Discovery to Clinical Applications*

Hendrikus H. Boersma, Bas L.J.H. Kietselaer, Leo M.L. Stolk, Abdelkader Bennaghmouch, Leonard Hofstra, Jagat Narula, Guido A.K. Heidendal and Chris P.M. Reutelingsperger

J Nucl Med. 2005;46:2035-2050.

The Journal of Nuclear Medicine is published monthly.
SNMMI | Society of Nuclear Medicine and Molecular Imaging
1850 Samuel Morse Drive, Reston, VA 20190.
(Print ISSN: 0161-5505, Online ISSN: 2159-662X)

SNMMI SOCIETY OF NUCLEAR MEDICINE AND MOLECULAR IMAGING